

Supporting Information

Bimetal-organic frameworks assisted polymerization of pyrrole involving air oxidant to prepare composite electrodes for the portable energy storage

Yang Jiao, Gang Chen, Dahong Chen, Jian Pei, Yongyuan Hu*

Corresponding Author

*Gang Chen

MIIT Key Laboratory of Critical Materials Technology for New Energy Conversion and Storage, School of Chemistry and Chemical Engineering, Harbin Institute of Technology, Harbin 150001, People's Republic of China

E-mail: gchen@hit.edu.cn

Phone: (+86)-0451-86413753



Fig. S1. Optical image of the Zn/Ni-MOF and Zn/Ni-MOF@PPy powder.

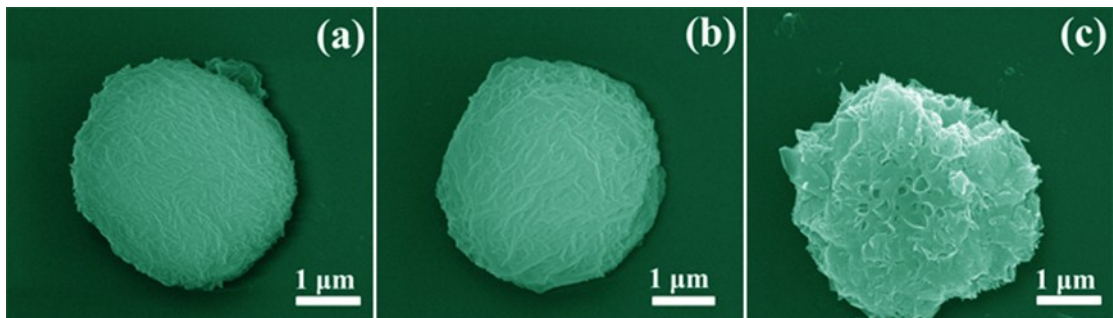


Fig. S2. The SEM images of (a) Zn/Ni-MOF@PPy-0.05, (b) Zn/Ni-MOF@PPy-0.1 and Zn/Ni-MOF@PPy-0.2.

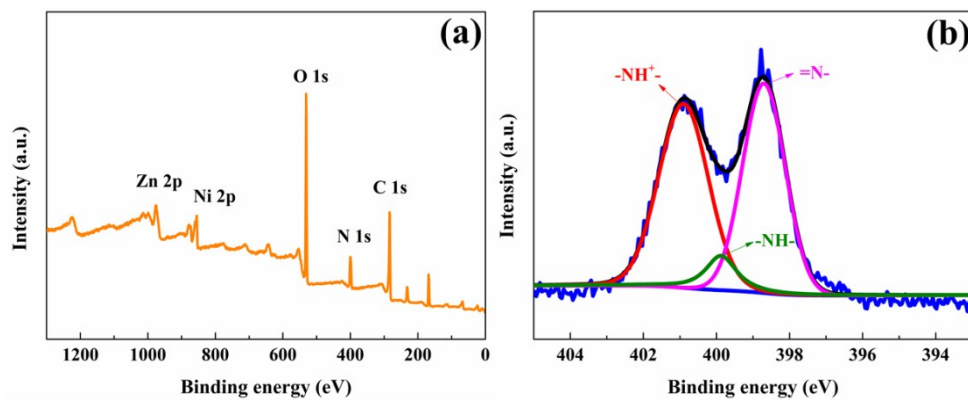


Fig. S3. (a) XPS spectra of Zn/Ni-MOF@PPy, (b) N1s.

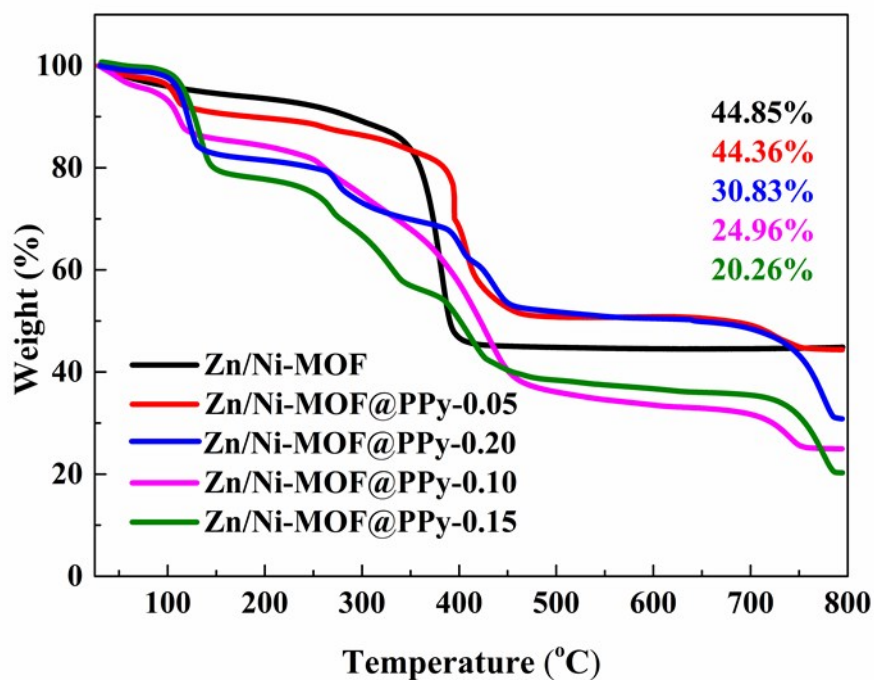


Fig. S4. The TGA curves of the Zn/Ni-MOF and Zn/Ni-MOF@PPy-n (n = 0.05, 0.10, 0.15, 0.20) composites.

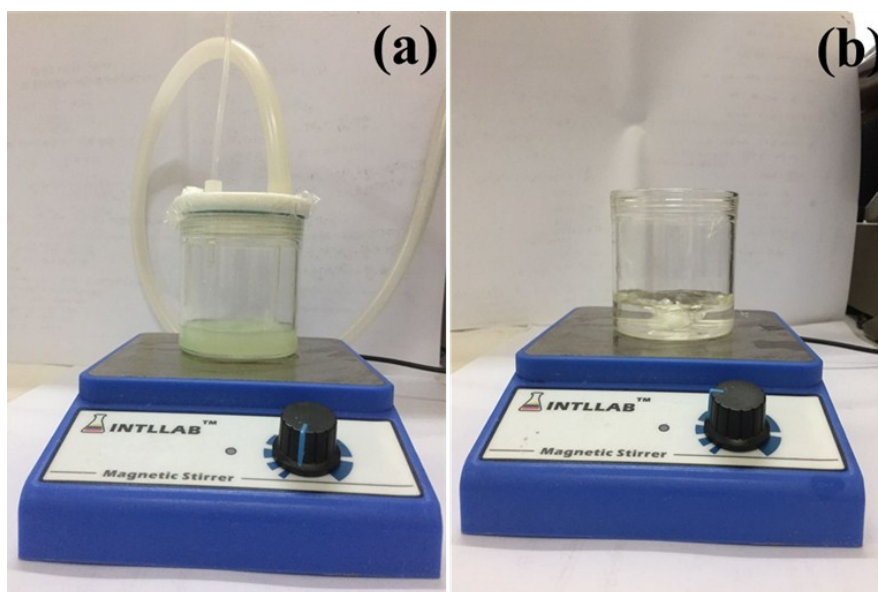


Fig. S5. The effects of different experimental conditions on the formation of polypyrrole: (a) Optical image of reaction system the under N_2 atmosphere, (b) Optical image of reaction system without Zn/Ni-MOF added
 The Fig. S5(a, b) show that reactions carried out at nitrogen atmosphere or without Zn/Ni-MOF added doesn't yielded black polymer, indicating lack of either O_2 or Zn/Ni-MOF is negative to PPy production.

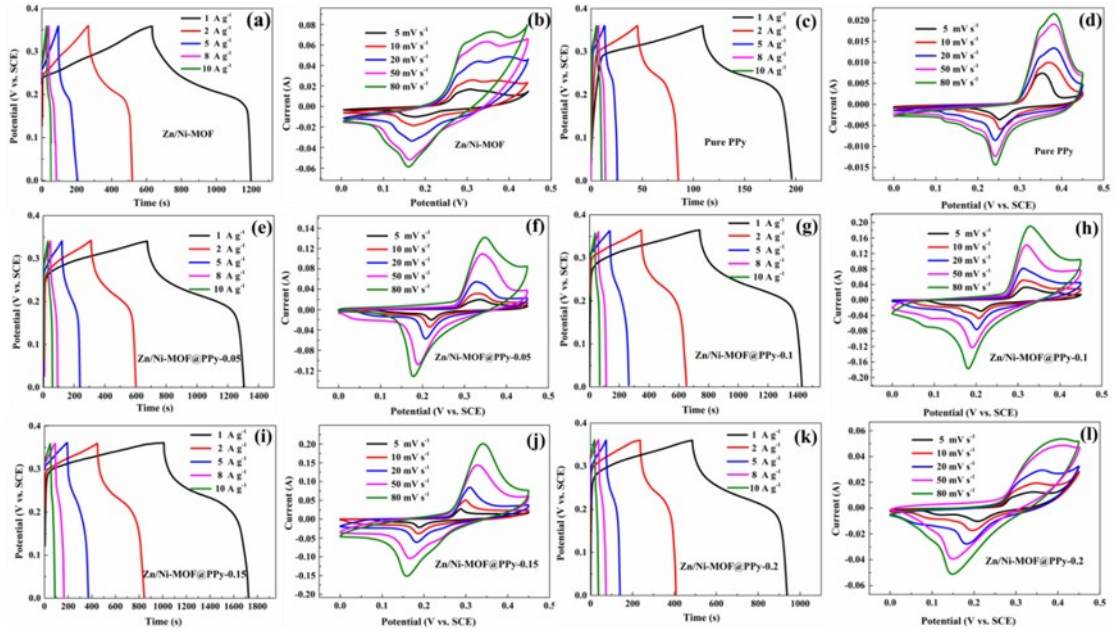


Fig. S6. (a, c, e, g, i, k) Charge-discharge curves of Zn/Ni-MOF and Zn/Ni-MOF@PPy-n ($n=0.05, 0.1, 0.15, 0.2$) at different current densities, respectively. (b, d, f, h, j, l) Cyclic voltammograms of Zn/Ni-MOF and Zn/Ni-MOF@PPy-n ($n=0.05, 0.1, 0.15, 0.2$) at different scan rates, respectively.

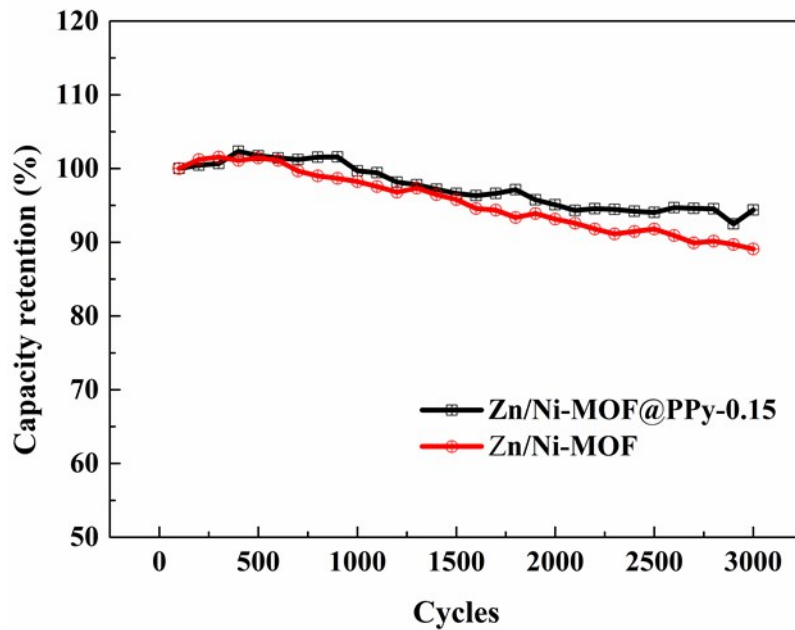


Fig. S7. Cycling performance of Zn/Ni-MOF@PPy-0.15 and Zn/Ni-MOF in three-electrode system.

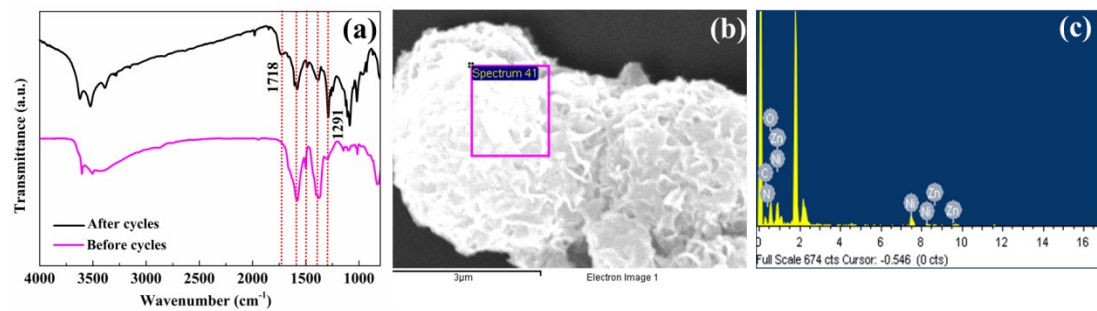


Fig. S8. (a) FTIR spectrum, (b) SEM image, (c) EDS of the Zn/Ni-MOF@PPy electrode after cycles.

For a comparative study, the electrochemical performance of Ni-MOF@PPy and Zn-MOF@PPy were also measured under the same condition (Fig. S8). Three-electrode cyclic voltammetry (CV) curves of Zn/Ni-MOF@PPy, Ni-MOF@PPy and Zn-MOF@PPy at the same scan rate were shown in Fig. S8a. The specific capacities correlated to the average areas of CV curves follow the order of Zn/Ni-MOF@PPy > Ni-MOF@PPy > Zn-MOF@PPy, indicating that more reactions occur in the Zn/Ni-MOF@PPy electrode. The galvanostatic charge-discharge curves (GCD) of the Co/Ni-MOF, Zn/Ni-MOF and Ni-MOF are shown in Fig. S8b. At the same current density, the Zn/Ni-MOF@PPy show a longest duration time for charging-discharging. The calculated specific capacities of Zn/Ni-MOF@PPy, Ni-MOF@PPy and Zn-MOF@PPy are 202.2, 124.5 and 70.9 mAh g⁻¹ at the current density of 1 A g⁻¹, respectively. Electrochemical impedance spectroscopy (EIS) was performed at a frequency range from 100 KHz to 0.01 Hz with a perturbation potential amplitude of 5 mV, as shown in Fig. S8c. The semicircle for Zn/Ni-MOF@PPy in the high frequency ranges is smaller than that of the Ni-MOF@PPy and Zn-MOF@PPy. A smaller semicircle indicates a smaller charge-transfer resistance (R_{ct}). The intercept of the real axis in the high frequency range of the Nyquist plots indicates the equivalent series resistance (ESR), which is the combined series resistance of the electrolyte, electrode, electrolyte and electrode contact resistance. It has also been found that the ESR of the different MOF@PPy follow the order of Zn/Ni-MOF@PPy > Ni-MOF@PPy > Zn-MOF@PPy. The synergistic effect between Zn/Ni-MOF and PPy is conducive to a remarkable enhancement in electrochemical performance.

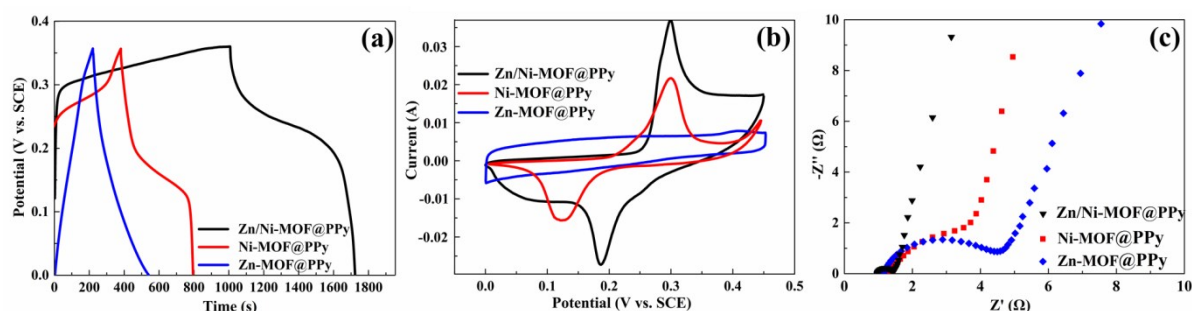


Fig. S9. (a) Charge and discharge curves (at 1 A g⁻¹), (b) The CV curves (at 5 mV s⁻¹), (c) Nyquist plots of the Zn/Ni-MOF@PPy, Ni-MOF@PPy and Zn-MOF@PPy.

For comparative study, the electrochemical performance of the physical mixture

of Zn/Ni-MOF and PPy (Zn/Ni-MOF+PPy) were also measured under the same condition (Fig. S9). Three-electrode cyclic voltammetry (CV) curves of Zn/Ni-MOF@PPy, Zn/Ni-MOF+PPy at the same scan rate were shown in Fig. S9a. The specific capacities correlated to the average areas of CV curves follow the order of Zn/Ni-MOF@PPy > Zn/Ni-MOF+PPy, indicating that more reactions occur in the Zn/Ni-MOF@PPy electrode. The galvanostatic charge-discharge curves (GCD) of the Zn/Ni-MOF@PPy and Zn/Ni-MOF+PPy are shown in Fig. S9b. At the same current density, the Zn/Ni-MOF@PPy show longer duration time for charging-discharging than the Zn/Ni-MOF+PPy. The calculated specific capacities of Zn/Ni-MOF@PPy and Zn/Ni-MOF+PPy are 202.2 and 165.4 mAh g⁻¹ at the current density of 1 A g⁻¹, respectively. Electrochemical impedance spectroscopy (EIS) was performed at a frequency range from 100 KHz to 0.01 Hz with a perturbation potential amplitude of 5 mV, as shown in Fig. S9c. The semicircle for the Zn/Ni-MOF@PPy in the high frequency ranges is smaller than that of the Zn/Ni-MOF+PPy. A smaller semicircle indicates a smaller charge-transfer resistance (R_{ct}). This indicates Zn/Ni-MOF@PPy composites may perform well as supercapacitor electrode material. For the Zn/Ni-MOF+PPy electrode material, the contact type between the Zn/Ni-MOF and PPy is “point contact”, as the conductive metrics can only contact the outer surface of the spherical flower; in contrast, the in situ polymerization method can ensure that the PPy layer extends into the Zn/Ni-MOF structure, making PPy and Zn/Ni-MOF to form a kind of “film contact”. Therefore, the electrochemical performance of Zn/Ni-MOF@PPy is preferable.

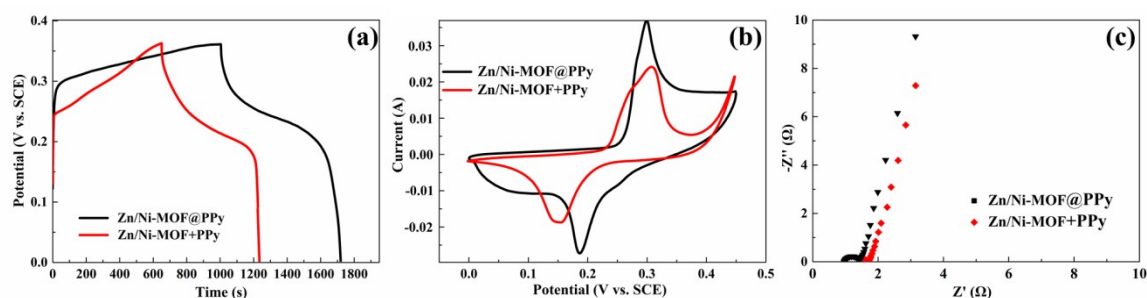


Fig. S10. (a) Charge-discharge curves (at 1 A g⁻¹), (b) The CV curves (at 5 mV s⁻¹), (c) Nyquist plots of the Zn/Ni-MOF@PPy and Zn/Ni-MOF+PPy.

Preparation of negative electrode and its electrochemical performances:

The negative electrode for the coin-type hybrid supercapacitor (HSC) was prepared by mixing Carbon nanotubes functionalized with carboxylic group (CNTs-COOH), carbon black, polyvinylene difluoride (PVDF) (in the weight ratio of 8:1:1) together using NMP as solvent. The mixture was coated onto the cleaned Ni foam (1 cm^2) and was kept for drying at $80 \text{ }^\circ\text{C}$ overnight. Then the electrode was used as the working electrode. 3 M KOH solution, saturated calomel electrode (SCE) and platinum foil were used as the electrolytes, reference and counter electrodes, respectively. The weight of active material is about 4 mg. The specific capacitance of CNTs-COOH is 138 F g^{-1} at the current density of 1 A g^{-1} (Fig. S11).

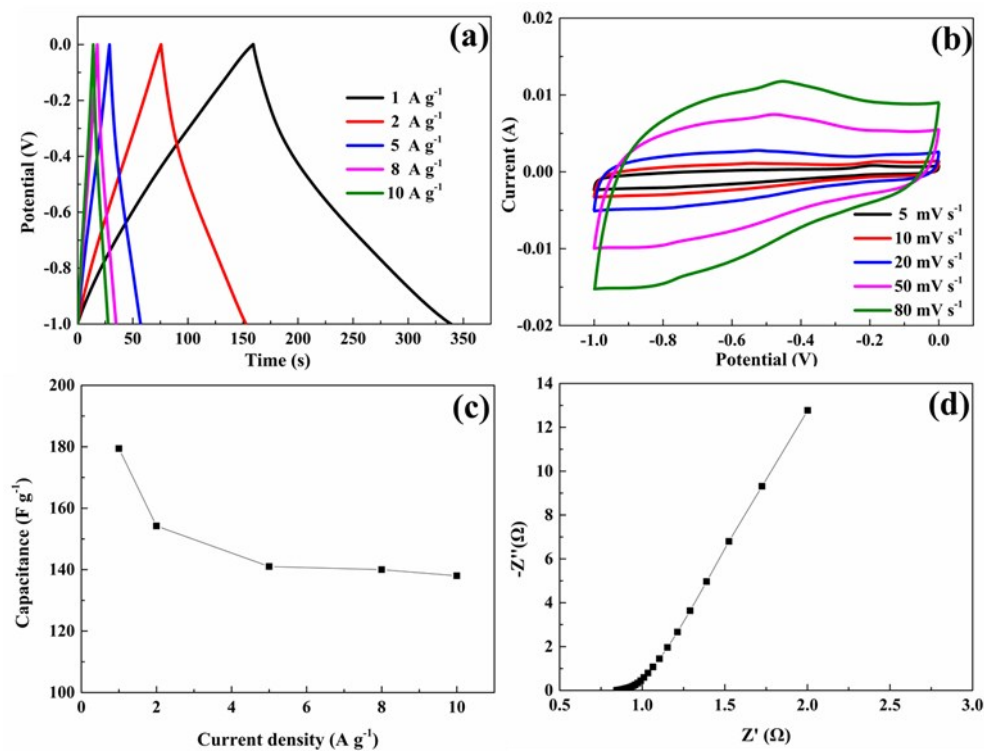


Fig. S11. (a) Charge and discharge curves of CNTs-COOH at different current densities ranged from 1 to 10 A g^{-1} , (b) CV curves of CNTs-COOH at the scan rate between 5 and 80 mV s^{-1} , (c) Specific capacity as a function of current density, (d) Nyquist plots of the CNTs-COOH.

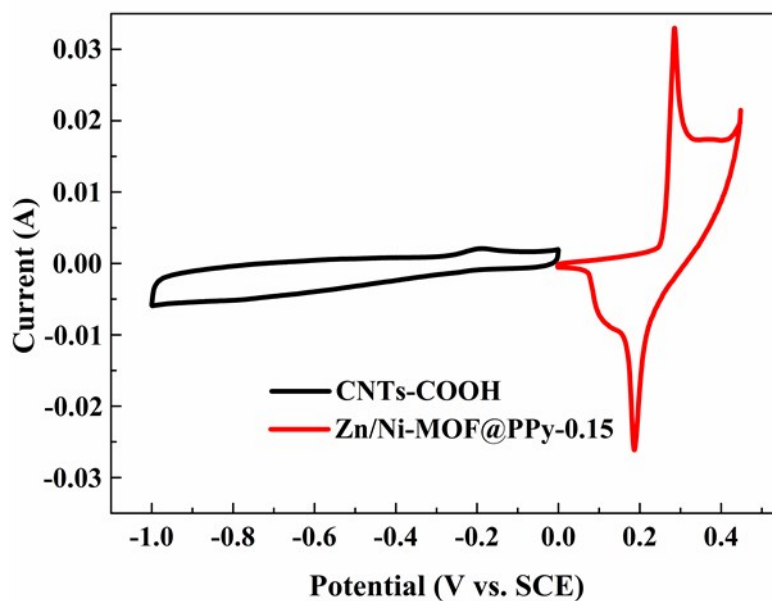


Fig. S12. (a) Cyclic voltammetry curves of the Zn/Ni-MOF@PPy and CNT-COOH electrodes performed in a three-electrode cell in a 3 M KOH electrolyte at a scan rate of 5 mV s^{-1} ;

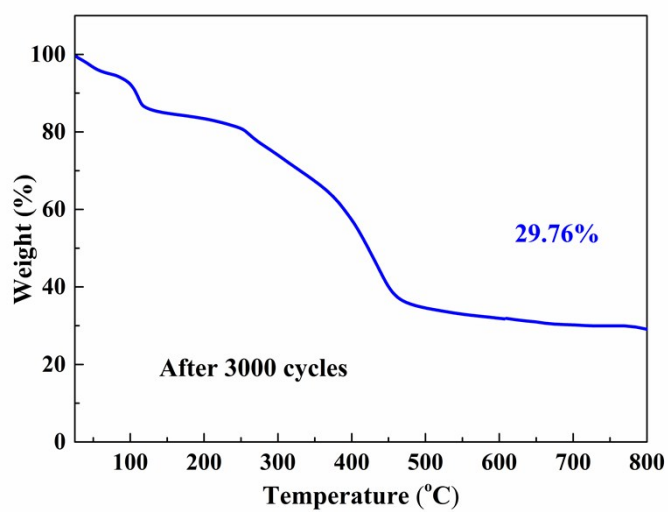


Fig. S13. The TGA curves of the Zn/Ni-MOF @PPy- 0.15 after cycles.

Table S1 Comparison of specific capacity among the previous reports and our works using the three-electrode system.

Electrode materials	Electrolyte	Current density (A·g ⁻¹)	Specific capacity (mAh·g ⁻¹)	Ref.
Ni-MOF (Ni ₃ (btc) ₂ ·12H ₂ O)	2 M KOH	1	80.6	S1
Ni-MOF nanorods [Ni(HOC ₆ H ₄ COO) _{1.4} ₈ (OH) _{0.52} ·1.1H ₂ O]	6 M KOH	2	283	S2
Accordion-like Ni-MOF [Ni ₃ (OH) ₂ (C ₈ H ₄ O ₄) ₂ (H ₂ O) ₄]·2H ₂ O	3 M KOH	0.7	182.3	S3
Ni-MOF [Ni ₃ (OH) ₂ (C ₈ H ₄ O ₄) ₂ (H ₂ O) ₄]·2H ₂ O	3 M KOH	1	123	S4
Zn/Ni-MOF [Ni ₃ - xZnx(OH) ₂ (C ₈ H ₄ O ₄) ₂ (H ₂ O) ₄]·2H ₂ O (X≈0.66)	3 M KOH	1	161.5	S5
Zn/Ni-MOF@PPy -0.05	3 M KOH	1	165.6	Our Work
Zn/Ni-MOF@PPy -0.10	3 M KOH	1	188.9	Our Work
Zn/Ni-MOF@PPy -0.15	3 M KOH	1	202.2	Our Work
Zn/Ni-MOF@PPy -0.20	3 M KOH	1	121.6	Our work

Table S2 Various performance parameters for our Zn/Ni-MOF@PPy-0.15//CNT-COOH coin-type Hybrid Supercapacitors

Current density (A·g ⁻¹)	Discharge Time (s)	Specific Capacity (F·g ⁻¹)	Energy density (W·h·kg ⁻¹)	Power density (W·kg ⁻¹)
1	285	203	55.3	699
2	137	187	50.9	1338
5	40.8	145	39.5	3485
8	22.8	130	35.4	5590
10	14.8	102	27.8	6762

Table S3 Comparison of electrochemistry performance of electrochemical energy stored devices fabricated in our work with others reported.

Electrode materials	Counter	Electrolyte	Potential Window (V)	Energy Density (W·h·Kg ⁻¹)	Power Density (W·Kg ⁻¹)	Ref.
SP@rGO	SP@rGO@Co	2 M KOH	1.5	33	800	S6
NiO	rGO	1 M KOH	1.7	39.9	360	S7
MWCNT/amor- Ni(OH) ₂ /PEDOT:PSS	rGO/CNT	1 M KOH	1.5	58.5	780	S8
Ni-MOF/CNT	rGO/C ₃ N ₄	6 M KOH	1.6	36.6	480	S9
Ni-MOF	CNTs-COOH	3 M KOH	1.4	49.7	700	S4
Zn/Ni-MOF	CNTs-COOH	3 M KOH	1.45	53.6	725	S5
Zn/Ni-MOF@PPy-0.15	CNTs-COOH	3 M KOH	1.4	55.3	699	Our work

SP: macroporous 3D sponge

MWCNT: multiwalled carbon nanotube

PEDOT:PSS: poly (3,4-ethylenedioxythiophene)-poly(styrenesulfonate)

rGO: reduced graphene oxide

CNT: carbon nanotube

CNTs-COOH: carbon nanotubes functionalized with carboxylic group

References

- [S1] L. Kang, S. Sun, L. Kong, J. Lang, Y. Luo, *Chin. Chem. Lett.*, 2014, **25**, 957-961.
[S2] J. Xu, C. Yang, Y. Xue, C. Wang, J. Cao and Z. Chen, *Electrochim. Acta*, 2016, **211**, 595-602.
[S3] Y. Yan, P. Gu, S. Zheng, M. Zheng, H. Pang and H. Xue, *J. Mater. Chem. A*, 2016, **4**, 19078-19085.
[S4] Y. Jiao, J. Pei, C. Yan, D. Chen, Y. Hu and G. Chen, *J. Mater. Chem. A*, 2016, **4**, 13344-13351.

- [S5] Y. Jiao, J. Pei, D.H. Chen, C.S. Yan, Y.Y. Hu, Q. Zhang, G. Chen, *J. Mater. Chem. A*, 2017, **5**, 1094-1101.
- [S6] D. P. Dubal, R. Holze, P. Gomez-Romero, *Sci. Rep.*, 2014, **4**, 7349–7358.
- [S7] F. Luan, G. Wang, Y. Ling, X. Lu, H. Wang, Y. Tong, X. X. Liu, Y. Li, *Nanoscale*, 2013, **5**, 7984-7990.
- [S8] W. C. Jiang, D. S. Yu, Q. Zhang, K. L. Goh, L. Wei, Y. L. Yong, R. R. Jiang, J. Wei, Y. Chen, *Adv. Funct. Mater.*, 2015, **25**, 1063-1073.
- [S9] Wen, P. et al. *J. Mater. Chem. A*, 2015, **3**, 13874-13883.